The Effect of Microstructure and Environment on Fatigue Crack Closure of 7475 Aluminum Alloy

R. D. CARTER, E. W. LEE, E. A. STARKE, Jr., and C. J. BEEVERS

The effects of slip character and grain size on the intrinsic material and extrinsic closure contributions to fatigue crack growth resistance have been studied for a 7475 aluminum alloy. The alloy was tested in the underaged and overaged conditions with grain sizes of 18 μm and 80 μm. The fracture surface exhibited increased irregularity and planar facet formation with increased grain size, underaging, and tests in vacuum. These changes were accompanied by an increased resistance to fatigue crack growth. In air the 18 μm grain size overaged material exhibited relatively poor resistance to fatigue crack growth compared with other microstructural variants, and this was associated with a lower stress intensity for closure. All materials exhibited a marked improvement in fatigue crack growth resistance when tested in vacuum, with the most significant difference being $\sim 1000\times$ at a ΔK of 10 MPa $m^{1/2}$ for the 80 μm grain size underaged alloy. This improvement could not be accounted for by either an increase in closure or increased crack deflection and is most likely due to increased slip reversibility in the vacuum environment. The intrinsic resistance of the alloy to fatigue crack growth was microstructurally dependent in vacuum, with large grains and planar slip providing the better fatigue performance.

I. INTRODUCTION

TRADITIONAL design of cyclically loaded components utilizes the fatigue endurance limit: a parameter experimentally determined using defect-free samples.[1] Lately, fracture mechanics concepts have been used in conjunction with nondestructive measurements of defects to establish the maximum cyclic stress below which a detectable crack will not grow.[2,3] The resulting design parameter used for the preexisting defect tolerant approach is the threshold stress intensity range, ΔK_{th}. Recent studies have shown that the magnitude of this experimentally determined parameter can be greatly influenced by closure effects. Elber[4] pointed out the existence of crack closure in 1970 when he observed that a crack in a fatigue specimen was closed during a portion of the loading cycle, even when the minimum load was tensile. Since crack closure always gives a positive effect, *i.e.*, it reduces fatigue crack growth rates, there is considerable interest in identifying the mechanisms associated with closure.

Fatigue crack closure was considered by early researchers to be only a plane stress phenomenon[5] caused by the restraint of elastic material surrounding permanent plastic tensile deformation left in the wake of the propagating crack,[4] and was termed "plasticity-induced crack closure."[6] Later, crack closure was found to be significant in thick specimens under plane strain conditions, and attributed to crack branching and Mode II displacements.[7] Closure resulting from mode II displacements requires a rough or uneven fracture surface and is termed "roughness-induced crack closure."[6] An oxidizing environment may also influence closure behavior, and Ritchie and Suresh[8] suggest that "oxide-induced crack closure" may occur during low crack growth rates where sufficient time is allowed for the formation of thick oxide layer which prevents the crack from closing when the load is removed.

Since closure reduces crack propagation rates it is of practical importance to determine those parameters which enhance its occurrence. Slip length and slip behavior have been shown to influence both the fracture path (crack branching and surface roughness) and environmental sensitivity of fatigue crack growth.[9-12] The purpose of this study was to investigate the roughness-induced and oxide-induced crack closure behavior of 7475 aluminum alloy under different microstructural and environmental conditions. Emphasis was placed on the effect of grain size and deformation mode on crack closure of compact tension samples subjected to plane strain conditions in a vacuum and in a laboratory air environment.

II. EXPERIMENTAL

The 7475 alloy used in this research was obtained as 2.5 inch thick plate from the Alcoa Technical Center. The chemical composition in weight percent is given in Table I. Starting with the 2.5 inch thick plate, two different intermediate thermomechanical treatments (ITMT's), shown schematically in Figure 1, were used to obtain the desired grain structure. They include solutionizing, overaging, warm rolling, and recrystallization treatments. The large particles (~ 1 μm diameter) that result from the overaging treatment create strain concentrations during the warm rolling, and these deformation zones act as nucleation sites for recrystallization.[13] Small grains were obtained by using a large amount of deformation and rapid heating to the recrystallization temperature (Figure 1(a)). Large grains were obtained by using a small amount of deformation and slow heating to the recrystallization temperature (Figure 1(b)). All heat treatments were conducted in a molten nitride salt bath except those associated with the rolling operation which were conducted in an electric air furnace. Samples

R. D. CARTER is an Engineer, United States Army Corps of Engineers, P.O. Box 61, Tulsa, OK 74121. E. W. LEE is a Postdoctoral Fellow, Fracture and Fatigue Research Laboratory, Georgia Institute of Technology, Atlanta, GA 30332. E. A. STARKE, Jr. is Earnest Oglesby Professor of Materials Science, Department of Materials Science, University of Virginia, Charlottesville, VA 22901. C. J. BEEVERS is Professor, Department of Metallurgy and Materials, University of Birmingham, Birmingham B15 2TT, England.

Manuscript submitted August 15, 1983.

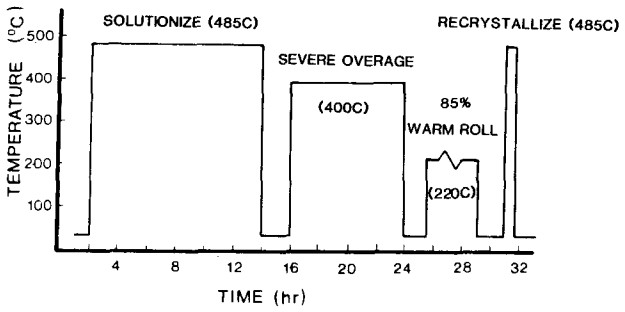

(*a*)

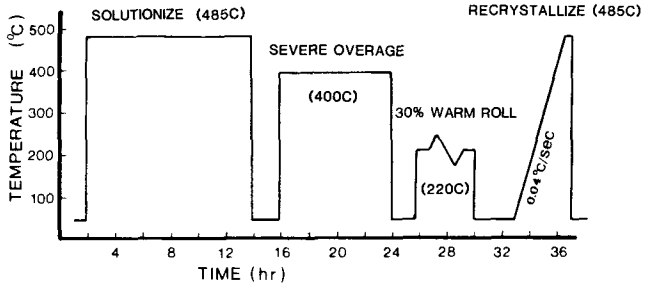

(*b*)

Fig. 1—Thermomechanical treatments used to obtain the recrystallized grain structure for 7475 Al alloy. (*a*) Processing for 18 μm grains, (*b*) processing for 80 μm grains.

Table I. Alloy Composition, Wt Pct

Cu	Zn	Mg	Ti	Fe	Si	Cr	Al
1.65	5.79	2.35	0.01	0.12	0.06	0.23	Bal.

were quenched in water from the recrystallization temperature, stretched approximately two percent to redistribute the residual quenching stresses, and naturally aged for three days. Samples for each grain size were artificially aged in an oil bath to obtain either an underaged or an overaged condition.

Metallographic samples were prepared using standard procedures and etched with Keller's reagent. The grain size was defined as the diameter, D_{eq}, of a sphere having an equivalent volume, V, of a rectangle determined from measured mean intercept lengths, $V = (L_1)(L_2)(L_3)$, and $D_{eq} = [(6/\pi)V]^{1/3}$. L_1, L_2, and L_3 are the mean intercept lengths from the short transverse, long transverse, and rolling plane, respectively. Crystallographic texture determinations were carried out using the reflection method. Fixed time increments were employed to collect intensity data over a polar orientation range from 0 to 70 degrees. A computer program was used to construct the pole figures in the form of equal value contours and provided average, maximum, and minimum intensities.

All mechanical tests were performed on a closed loop servohydraulic machine. The specimens were taken from the central portions of the plates with the stress axes parallel to the rolling (longitudinal) direction, and the notch (for the fcp specimens) normal to the rolling direction. The tensile specimens conformed to ASTM E8-69 and were tested at a strain rate of 10^3 per second in laboratory air using a clip-on extensometer. Crack propagation tests were conducted in both laboratory air with a relative humidity of 50 pct and vacuum at 10^{-6} torr, both at a temperature of ~22 °C, using compact-tension specimens (H/W = 0.486, thickness = 7.1 mm), an R ratio of 0.1, and a frequency of 30 Hz. The crack propagated in the long-transverse direction on a plane normal to the rolling direction (L-T orientation). Crack lengths were measured to an accuracy of 0.01 mm on the polished surface of the specimen using a Gaertner traveling microscope. Crack closure was measured at 0.2 Hz from plots of load *vs* displacement (Figure 2), which were automatically recorded using a clip-on displacement gage. When the fracture surfaces separate, a change in compliance occurs, and the closure load is taken at this juncture (Figure 2). All da/dN and closure measurements were made in the region $a/w = 0.5$ to eliminate the effect of crack length dependence of crack closure.

SEM was used to examine the fracture features. Thin foils were prepared from the gage sections of tensile specimens for TEM studies of the deformation behavior.

III. RESULTS

A. *Microstructure*

The ITMT of Figure 1(a) produced a completely recrystallized, small equiaxed grain structure (Figure 3(a)), with D_{eq} = 18 μm. The ITMT of Figure 1(b) produced a completely recrystallized large, slightly elongated, grain structure (Figure 3(b)), with D_{eq} = 80 μm. Pole figures generated from X-ray diffraction data indicated that both materials had a random texture—an expected result since the recrystallization nuclei formed in the deformation zones associated with coarse precipitates located randomly throughout the matrix.

B. *Monotonic Properties*

Two aging treatments having equivalent hardness values (Figure 4) but different types of precipitates were selected for tensile and fcp studies. Underaging 7475 produces

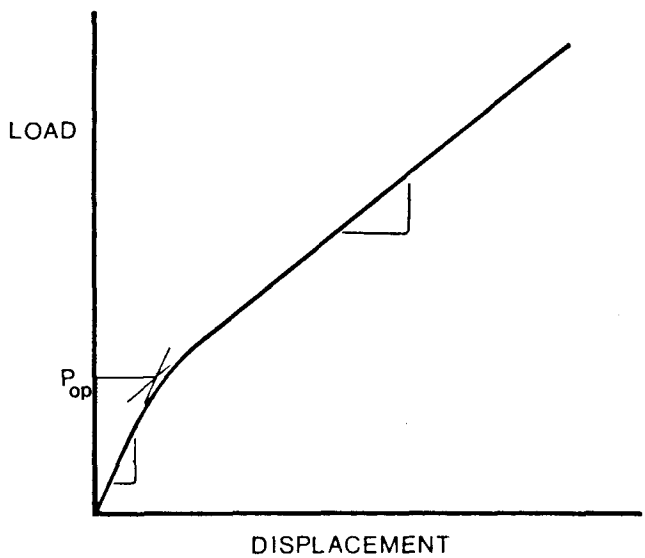

Fig. 2—Typical closure curve showing the change in compliance of the specimen due to the fracture surfaces separating. The opening load is taken at the intersection of the 2 slopes.

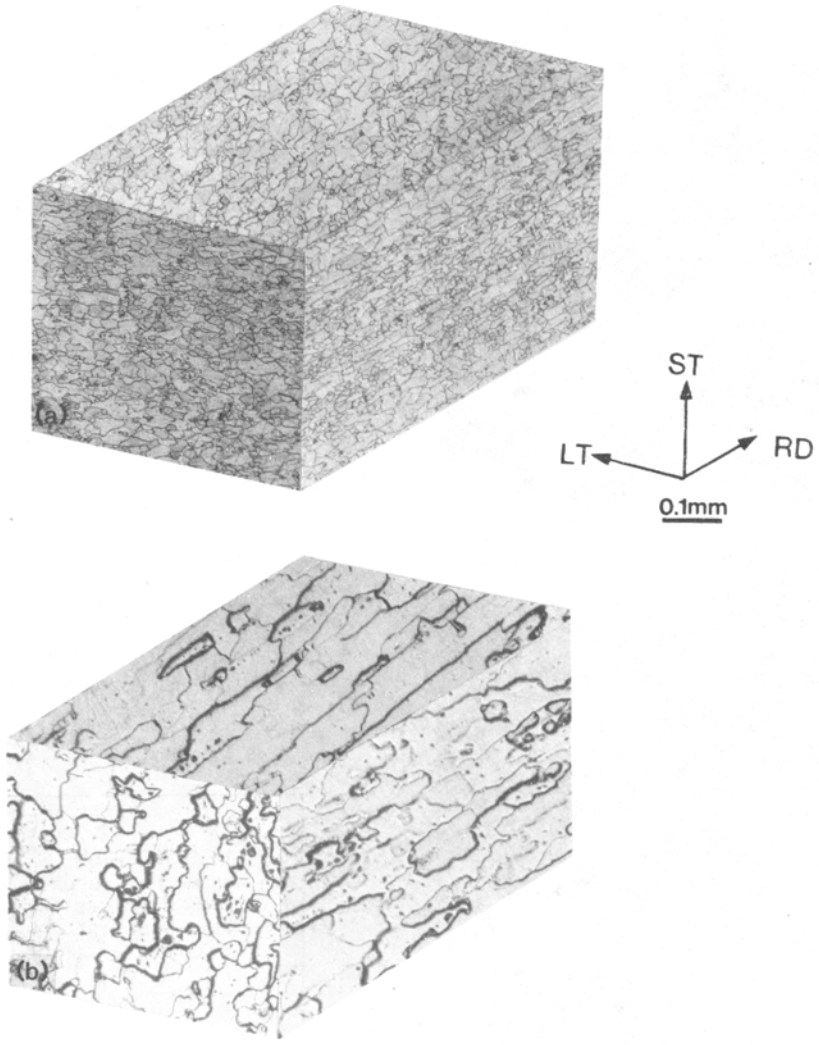

Fig. 3—Optical micrographs of ITMT 7475 (*a*) D_{eq} = 18 μm, (*b*) D_{eq} = 80 μm. D_{eq} is the diameter of a sphere of equivalent volume.

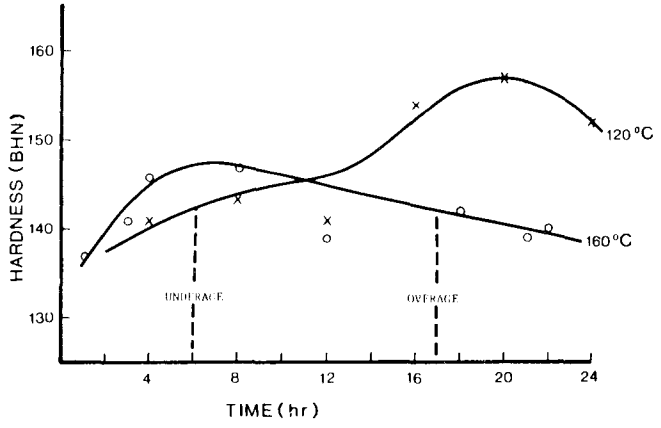

Fig. 4—Aging curves for 7475 alloy at 120 °C and 160 °C indicating times and temperatures used for the underaging and overaging treatments.

coherent precipitates which are sheared by dislocations resulting in planar slip (Figure 5(a)). Overaging produces incoherent precipitates which are looped and bypassed by dislocations resulting in wavy slip (Figure 5(b)). The yield strengths for the four experimental conditions (underaged and overaged, small and large grains) are listed in Table II. Reducing the grain size by a factor of ~4 for the underaged condition increases the strength by 54 MPa. This increase is due to a small Hall-Petch contribution since the precipitates are sheared, the texture is random, and the slip length is determined by the grain size.[14] However, the strength is independent of grain size for the overaged condition since the precipitates are looped and the slip length is determined by the interparticle spacing.

C. *Fatigue Crack Growth Data*

The fatigue crack growth response was investigated over the growth rate range $\sim 10^{-10}$ m/cycle to $\sim 10^{-6}$ m/cycle. The results obtained from 18 and 80 μm grain size material in the underaged and overaged condition and tested in laboratory air are presented in Figure 6. For growth rates less than $\sim 10^{-8}$ m/cycle the overaged material exhibited less resistance to fatigue crack growth and lower "thresholds". The 18 μm grain size overaged material exhibited higher crack growth rates than the other materials investigated.

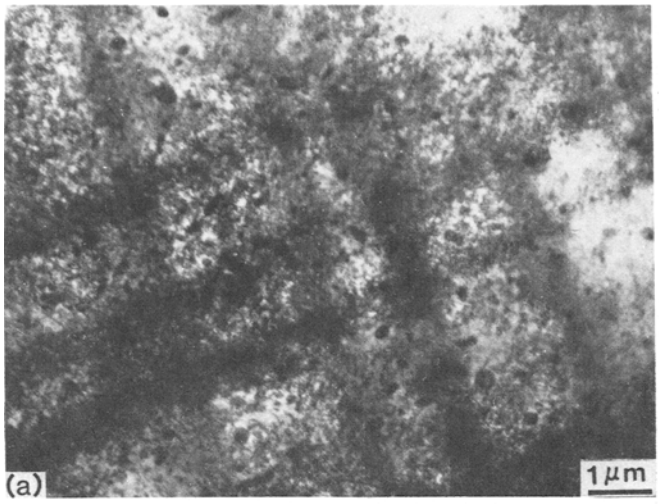

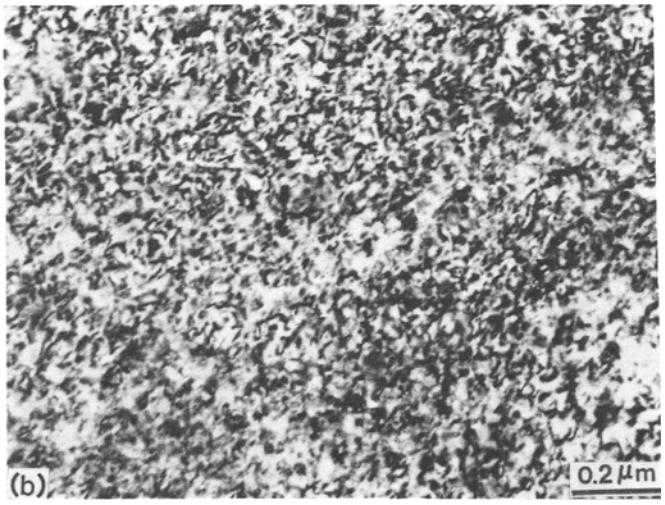

Fig. 5—TEM's showing the slip character for (*a*) the underaged treatment–planar deformation and (*b*) the overaged treatment–homogeneous deformation.

Table II. Yield Strength

18 μm Grain Size	Yield Strength (MPa)
underaged	505
overaged	455
80 μm Grain Size	
underaged	451
overaged	445

For tests carried out in vacuum there was a significant increase in fatigue crack growth resistance as illustrated in Figure 7. Data points are shown in this figure to illustrate the scatter associated with the tests. For the overaged alloy the crack growth rates at a ΔK of 7 MPa $m^{1/2}$ were reduced by a factor of ~10 in vacuum compared with an air test environment. For the 80 μm grain size underaged alloy the fatigue crack growth resistance improved by a factor of >100 for a vacuum test environment. Both of the underaged alloys exhibited slower fatigue crack growth rates than the overaged alloys.

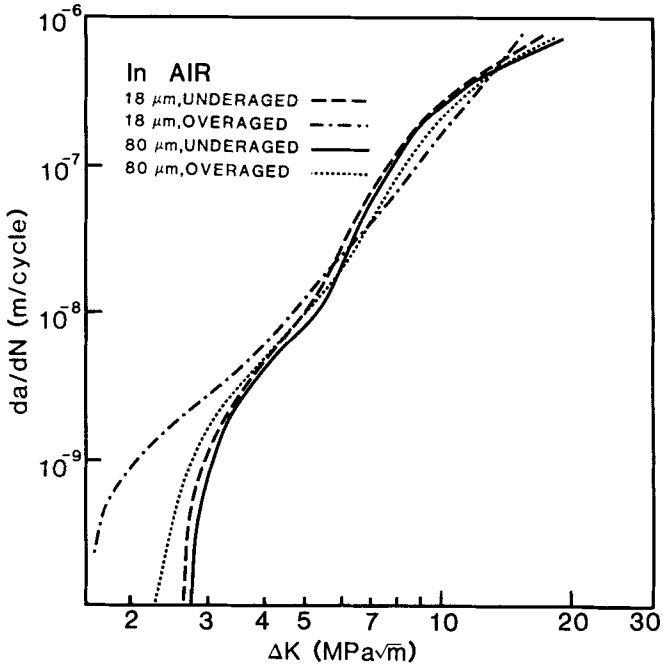

Fig. 6—FCGR's of the microstructural variants of 7475 tested in laboratory air.

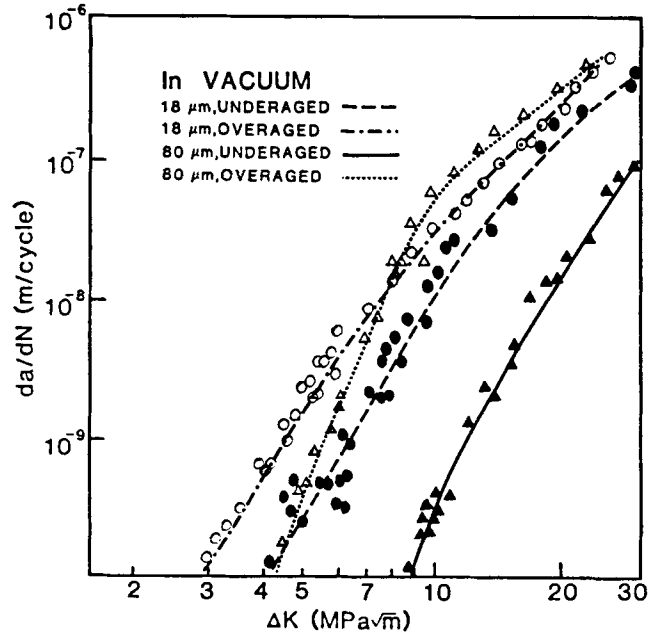

Fig. 7—FCGR's of the microstructural variants of 7475 tested in vacuum.

The crack closure response of the CT specimens was measured and a load P_{op} was identified. By incorporating the load range P_{max} to P_{op} into the computation of ΔK a range of values of ΔK_{eff} was obtained. The results obtained for ΔK_{eff} are included in Figures 8 and 9 for the air and vacuum tests, respectively. In both air and vacuum, crack closure had occurred and the magnitude of the closure stress intensity was between 1 to 2 MPa $m^{1/2}$ for all materials. The fatigue crack growth curves in air were brought together by a ΔK_{eff} plot, but in vacuum the large difference in growth rate remained and the materials maintain a high degree of resistance to fatigue crack growth.

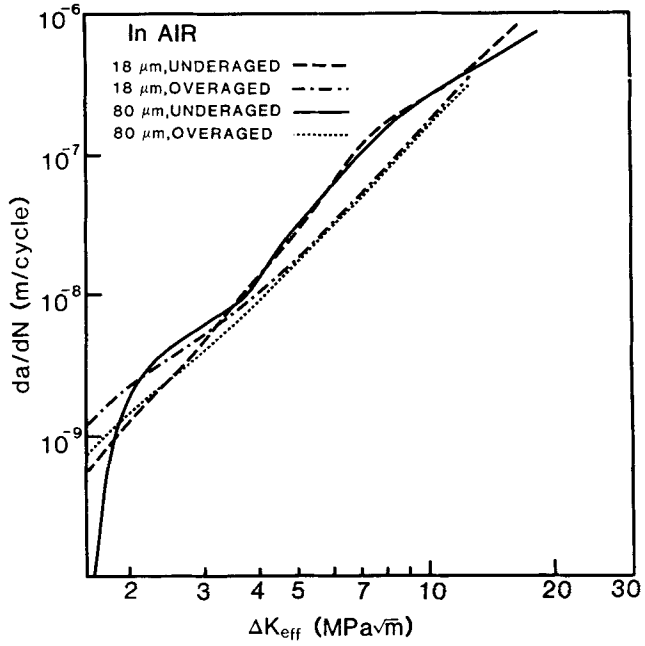

Fig. 8—FCGR's of the laboratory air tests as a function of the stress intensity range after correcting for closure.

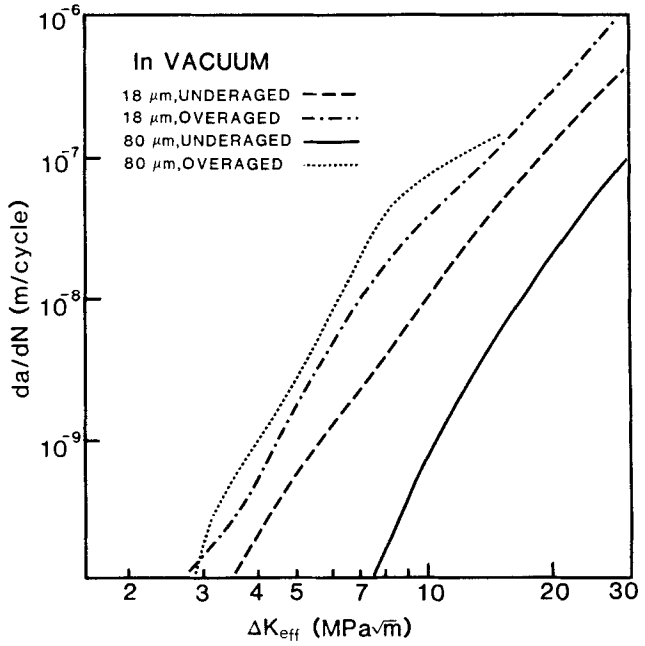

Fig. 9—FCGR's of the vacuum tests as a function of stress intensity range after correcting for closure.

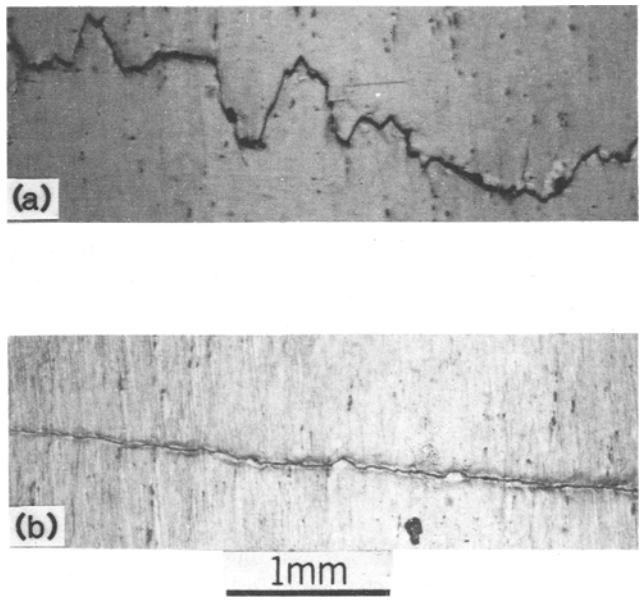

Fig. 10—Optical micrographs showing the crack paths of the 80 μm grain size 7475 tested in vacuum (*a*) underaged condition, (*b*) overaged condition.

D. *Fatigue Crack Path*

Examination of the fatigued but not completely broken test pieces at a macro level (magnification 25 times) revealed that the crack trajectory was nonplanar, and the extent of out of plane displacement of the crack increased with grain size and for the underaged condition. The most irregular crack path was observed in the 80 μm underaged alloy tested in vacuum (Figure 10(a)), and can be compared with a crack profile for an 80 μm grain size overaged alloy also tested in vacuum (Figure 10(b)). Examination of the fatigue fracture surface profiles in the SEM revealed an irregular fracture path for all alloys. The fracture features for the underaged and overaged 80 μm grain size material tested in air and vacuum are presented in Figures 11(a) to (d). The photographs were taken near the specimen surface, but are representative of through-thickness features. The features for both air tests were similar and not unlike those for the overaged condition tested in vacuum. Similar results were obtained for the 18 μm grain size material. The out-of-plane character of the crack was most marked in the 80 μm grain size underaged material tested in vacuum.

E. *Fracture Surface Morphology*

The fracture surface indicated a mixed mode of separation with facet formation on crystallographic planes and transgranular ductile separation with some striation formation. Facet formation occurred in both air and vacuum tests and in the underaged and overaged alloys.

A comparison of the effect of aging condition and grain size on the fracture surface morphology and mode of fatigue crack growth is presented in Figures 12(a) to (d). In the threshold region all the alloys exhibited faceted crack growth. The size of the facets and the propensity of their formation was clearly most marked in the 80 μm grain size underaged alloy.

IV. DISCUSSION

The present results are consistent with earlier studies that showed that slip character[10] and grain size[9] can have a pronounced effect on the fatigue crack growth behavior of age hardenable aluminum alloys. When the strengthening precipitates are coherent with the matrix (underaged condition) they are sheared by dislocations promoting coarse planar slip and inhomogeneous deformation. This favors fracture

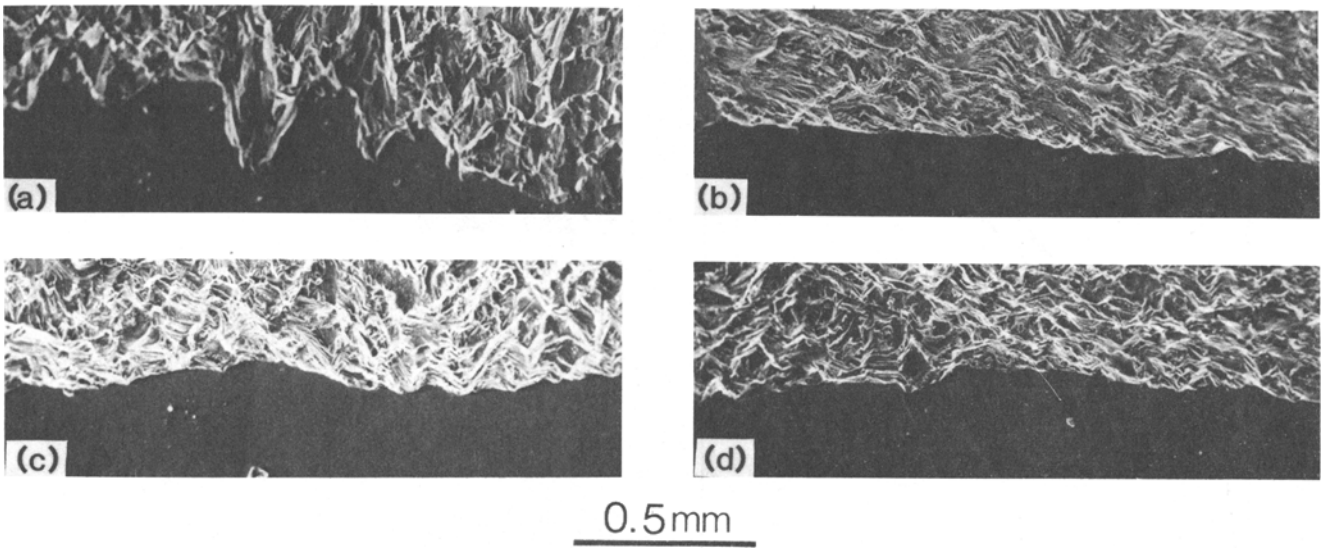

Fig. 11—SEM's showing the crack path and fracture features in the threshold region for the 80 μm grain size 7475 (*a*) underaged, tested in vacuum, (*b*) overaged, tested in vacuum, (*c*) underaged, tested in air, and (*d*) overaged, tested in air.

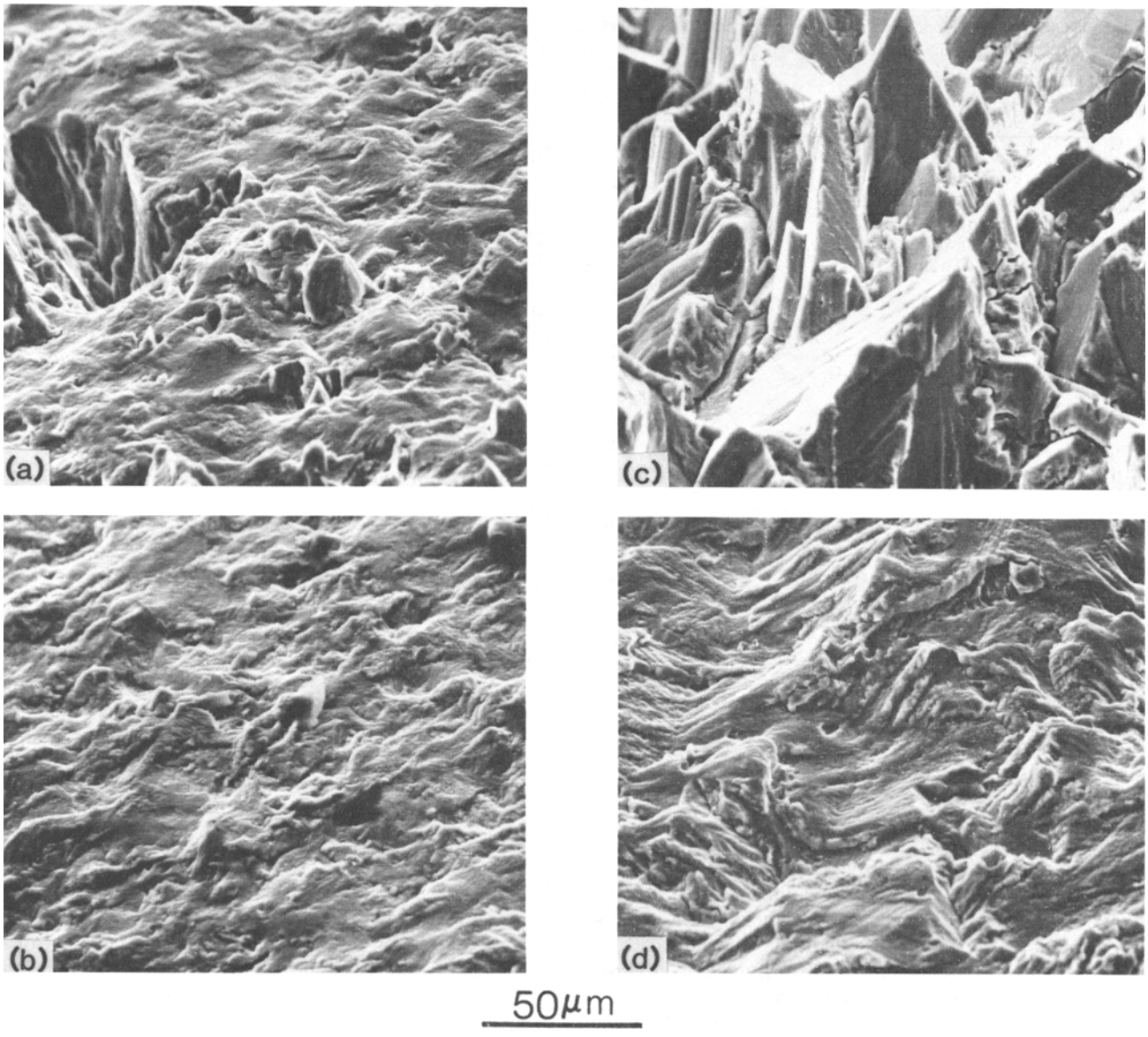

Fig. 12—SEM's of the FCP fracture features near threshold tested in vacuum (*a*) underaged 18 μm grain size, (*b*) overaged 18 μm grain size, (*c*) underaged 80 μm grain size, and (*d*) overaged 80 μm grain size.

along slip planes and the occurrence of zigzag crack growth and crack branching. When the strengthening precipitates are incoherent with the matrix (overaged condition), they are looped and bypassed by dislocations promoting more homogeneous deformation and reducing crack tortuosity. A reduction in grain size (by enhancing multiple slip at low ΔK's[9]) and an aggressive environment (by decreasing the plasticity needed for fracture[15]) can also reduce crack tortuosity although the oxides formed in air can have an opposite effect on crack growth rates by contributing a closure component. The slower crack growth rates associated with planar slip and large grains have been attributed to: (a) slip being more reversible,[9] (b) the tortuosity of the crack path,[10] (c) the ΔK of zigzag and branched cracks being smaller than the ΔK calculated assuming a single crack normal to the stress axis,[10] and (d) enhanced closure associated with increased surface roughness.[16]

A reduction in grain size, overaging, and an air environment reduces the reversibility of slip and crack tortuosity. Consequently, it is not surprising that the 18 μm grain size, overaged material had the poorest fatigue resistance of all the conditions studied. A comparison of Figures 6 and 8 suggests that the differences in fatigue crack growth rates for the various materials may be related to the difference in the extent of crack closure that they exhibited in the air environment. However, this is probably an oversimplification of microstructure-closure-FCP relationship. Figure 13 shows the variation in U with ΔK for all materials tested in laboratory air, where

$$U = \frac{K_{max} - K_{cl}}{\Delta K}$$

It is obvious that the difference in closure between the 18 μm grain size overaged material and the other microstructural variant is essentially constant up to a ΔK of ~8 MPa $m^{1/2}$ although the growth rates converge at ~4 MPa $m^{1/2}$. This may be due to an environmental contribution which is independent of closure. Lin and Starke[11,12] have shown that environmentally enhanced crack growth is greater for underaged than for overaged Al-Zn-Mg alloys and may also increase with increasing grain size. This could account for the convergence in crack growth curves even though the difference in closure contribution is maintained.

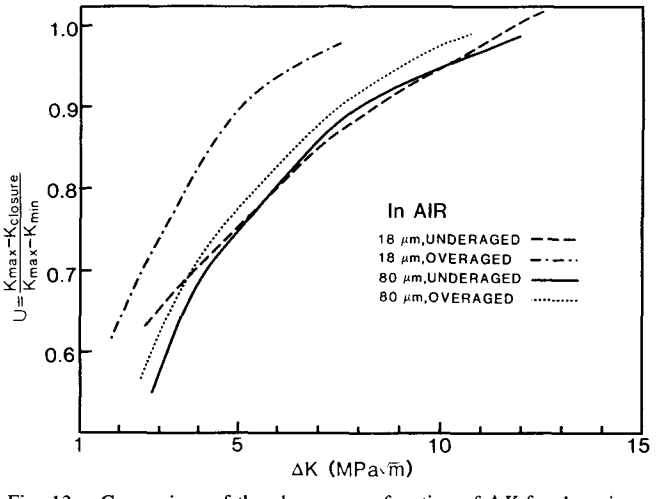

Fig. 13—Comparison of the closure as a function of ΔK for the microstructural variants tested in air.

One other observation should be noted here. The closure contribution is smaller for the overaged than for the underaged small grain size material. Vasudévan and Suresh[17] have shown that the oxide layer formed during fatigue of 7075 in air is thicker for overaged than for underaged materials. This fact in conjunction with our results indicates that the measured closure for the underaged alloy is not primarily due to oxides.

The creation of the asperities which resulted in the closure can be attributed to out of plane crack trajectories,[7] *i.e.*, roughness induced closure. The magnitude of the out of plane crack trajectory may be related to the ratio of the true crack length to the projected crack length, which for lack of a better term, we will define as the roughness parameter. The order of crack growth resistance is directly related to the magnitude of the closure component (Figure 13) and the roughness parameter (Table III).

The results of the vacuum studies were quite unlike those in air in that the differences in growth rates for the various materials could not be accounted for by closure effects (Figure 9). The influence of environment and in particular the improvement in fatigue crack growth resistance in vacuum has been observed in a range of aluminum alloys.[9-12,18] The extent of the improvement depends on aging condition and grain size, with the most significant improvements derived from coarse grained material in an underaged condition. Examination of Figure 7 shows that a similar response was achieved for the 7475 alloy. One factor which may account for this is the marked extent of slip reversibility in the underaged material compared with the multiple slip situation in the overaged material. An indication of the slip reversibility may be that the closure for the large grained UA material in vacuum and in air was the same (compare the U values in Figures 13 and 14 at ΔK = 10 MPa $m^{1/2}$) even though the fracture surface from the vacuum test was considerably rougher than the air test. Reversible slip would decrease the Mode II displacement during unloading and therefore the component of roughness induced closure. Reversible slip should also increase the number of cycles necessary to produce unit crack extension along a Mode II plane.

The crack closure that occurred in vacuum is represented in Figure 14 as variations in U, for the different materials, as a function of ΔK. The 18 μm overaged alloy showed no detectable closure at a ΔK of 5 MPa $m^{1/2}$. The increase of K_{cl} in air for this overaged material may be a consequence of oxide layer build-up (oxide induced closure) or alternately a consequence of a more irregular crack path and to microstructurally originated asperities, although the latter appear unlikely since the fracture surfaces and roughness parameter from the air and vacuum tests were similar for this

Table III. Roughness Parameter

Condition	True Length/Projected Length	
	Vacuum	Air
18 μm grain size		
UA	1.13	1.14
OA	1.05	1.05
80 μm grain size		
UA	1.67	1.18
OA	1.09	1.09

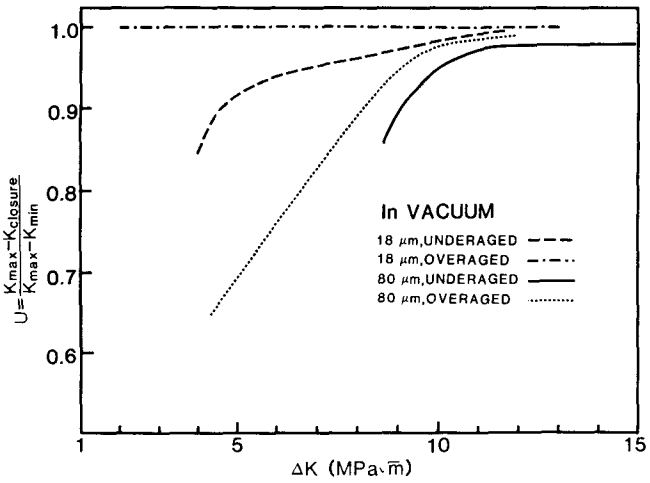

Fig. 14—Comparison of the closure as a function of ΔK for the microstructural variants tested in vacuum.

microstructure. Figure 14 also shows that the closure contribution was greater for both the underaged and overaged 80 μm grain size than for the underaged 18 μm grain size material. The closure is most likely associated with microstructurally originated asperities that result from the out of plane crack trajectories and Mode II displacements (roughness induced closure)[7] particularly since alternatives such as oxides and plasticity induced closure are absent for the vacuum tests at low ΔK levels. Although the roughness parameter of the underaged 18 μm grain size material was slightly larger than that for the overaged 80 μm grain size material, the closure was smaller. This is probably a consequence of slip being more reversible in the UA material.

The results in Figure 9 show that a marked difference exists between the intrinsic resistance of the 7475 alloy in the overaged and underaged condition. At a ΔK of 10 MPa $m^{1/2}$ the 80 μm underaged alloy exhibits a growth rate nearly 100× slower than the 80 μm overaged alloy, and both underaged alloys exhibit greater fatigue crack growth resistance than the overaged alloys. Comparison of the fractographs and crack profiles (Figures 10 to 12) illustrates that the underaged 80 μm grain size material exhibited marked surface irregularities and the crack advance involved both Mode I and II crack tip opening. Suresh[19] has suggested the following relationship for a deflected crack with a Mode II component (Figure 15):

$$\frac{d\bar{a}}{dN} = \left(\frac{D\cos\Theta + S}{D + S}\right)\left(\frac{da}{dN}\right)$$

Θ denotes the angle of deflection, D the distance over which the tilted crack advances along the kink, and S the distance over which linear (Mode I) crack growth occurs. $(d\bar{a}/dN)$ is the measured averaged growth rate of a deflected crack in each segment and (da/dN) the growth rate of an undeflected crack. For the 80 μm underaged alloy tested in vacuum $\Theta = 70$ deg and $S = 0.1\,D$. Using Suresh's analysis, the deflected crack has a 2.5 times slower growth rate compared with the undeflected crack. While a contributing factor, crack branching does not appear to be the complete explanation of the wide variations in fatigue crack growth rate presented in Figure 9.

There are several other possible explanations of this behavior, but these are qualitative in character. There is clearly

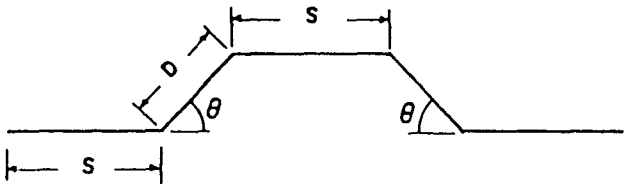

Fig. 15—Model profile of a segment of a deflected crack with the associated nomenclature (after S. Suresh[19]); see text for detailed description.

(Figures 11(a) and 12(c)) extensive out of plane crack growth with significant proportions of the crack advance under Mode II displacements. If the crack extension rates for equivalent displacements are less under Mode II than Mode I, then the crack profiles developed in the 80 μm underaged alloy would lead to a decrease in growth rate. A further point for consideration is the interaction of the fracture planes behind the crack tip. On the unloading part of the cycle the cracks may be pushed into firm contact as they attempt to slide over one another due to the reversible nature of the Mode II displacement for this microstructure. Only the 80 μm grain size material maintains the reverse and maximum plastic zone size less than the grain size at $\Delta K = 10$ MPa $m^{1/2}$. Sliding contact may well lead to friction welding of part of the crack faces with a subsequent reduction in the crack extension force. The friction welding together of fresh metal surfaces in vacuum under nonfatigue conditions is a well-established phenomenon; however, the extent of its role in this particular case cannot be quantified.

Some observations on the differences between the air and vacuum tests are appropriate. The 80 μm grain size underaged alloy has a growth rate 1000 times slower in vacuum than air at a ΔK of 10 MPa $m^{1/2}$. This outstanding difference is related to the factors previously discussed in relation to the behavior in vacuum. The other alloys exhibit the modest differences in fatigue crack growth rate up to a factor of 10 that might be expected for air and vacuum tests. The decrease in fatigue crack growth rate in vacuum may be attributed to the absence of an oxide layer in the crack tip region allowing slip reversibility to inhibit more effectively the crack extension process. The vacuum also excludes the presence of water vapor and other gases which could lead, for example, to hydrogen embrittlement of the material in the crack tip process zone and subsequently increase in the crack extension rate.

V. CONCLUSIONS

1. The fatigue crack growth resistance of a 7475 aluminum in laboratory air is improved with a coarse grain microstructure and in an underaged condition. This improvement can be directly correlated with an increase in the magnitude of the stress intensity for crack closure.
2. The fatigue crack growth resistance is greater in vacuum than in air. It seems likely that this is due to the absence of environmental embrittlement of the process zone and to the clean metal surfaces in the crack tip region allowing ease of slip reversibility.
3. In vacuum the alloys exhibited crack closure, similar in magnitude to that experienced in air. In vacuum the closure process was attributed to asperities formed on the

fatigue fracture surfaces as a consequence of facet formation and out of plane crack trajectories. An expected large increase in closure due to a very large increase in surface roughness for the 80 μm underaged material was not observed due to the reversibility of the Mode II displacement for this microstructure.

4. In vacuum the 80 μm grain size underaged alloy exhibited highly irregular crack profiles and fatigue crack growth rates up to 100 times slower than the 18 μm underaged and 80 μm overaged materials. This high degree of surface irregularity is attributed to the coarse grain size and planar slip characteristics of the underaged alloy.
5. The much greater fatigue crack growth resistance in vacuum of the 80 μm underaged alloy is considered to be a consequence of a number of factors including crack branching, mixed Mode I and II crack advance, enhanced slip reversibility, and possibly welding of the fracture surfaces on the unloading part of fatigue cycle.

ACKNOWLEDGMENTS

This research was sponsored by the Air Force Office of Scientific Research, United States Air Force Systems Command, under Grant AFOSR-83-0061, Dr. Alan H. Rosenstein, program manager. We would like to thank Dr. S. Suresh for furnishing us with a copy of his paper on crack deflection prior to publication.

REFERENCES

1. J. E. Shigley: *Mechanical Engineering Design*, 1977, McGraw-Hill, New York, NY, p. 179.
2. R. A. Smith: in *Fatigue Thresholds, Fundamentals and Engineering Applications*, J. Bäcklund, A. F. Blom, and C. J. Beevers, eds., Engineering Materials Advisory Services, Ltd., West Midlands, UK, 1981, vol. I, p. 33.
3. P. Stenvall: in *Fatigue Thresholds, Fundamentals and Engineering Applications*, J. Bäcklund, A. F. Blom, and C. J. Beevers, eds., Engineering Materials Advisory Services, Ltd., West Midlands, UK, 1981, vol. II, p. 931.
4. W. Elber: *Eng. Fracture Mech.*, 1970, vol. 2, p. 37.
5. T. C. Lindley and C. E. Richards: *Mat. Sci. Eng.*, 1974, vol. 14, p. 381.
6. R. O. Ritchie, S. Suresh, and C. M. Moss: *J. Eng. Mat. and Tech.*, Trans. ASME Series H, 1979, vol. 102, p. 293.
7. N. Walker and C. J. Beevers: *Fat. of Eng. Mat. and Struct.*, 1979, vol. 1, p. 135.
8. R. O. Ritchie and S. Suresh: *Metall. Trans. A*, 1978, vol. 9A, p. 291.
9. J. Lindigkeit, G. Terlinde, A. Gysler, and G. Lütjering: *Acta Metall.*, 1979, vol. 27, p. 1717.
10. Fu-Shiong Lin and E. A. Starke, Jr.: *Mat. Sci. Eng.*, 1980, vol. 43, p. 65.
11. Fu-Shiong Lin and E. A. Starke, Jr.: *Mat. Sci. Eng.*, 1980, vol. 45, p. 153.
12. Fu-Shiong Lin and E. A. Starke, Jr.: in *Hydrogen in Metals*, A. W. Thompson and I. M. Bernstein, eds., TMS-AIME, Warrendale, PA, 1981, p. 485.
13. John A. Wert, N. E. Paton, C. H. Hamilton, and M. W. Mahoney: *Metall. Trans. A*, 1981, vol. 12A, p. 1267.
14. Edgar A. Starke, Jr.: *Strength of Metals and Alloys (ICSMAG)*, R. C. Gifkins, ed., Pergamon Press, Oxford, 1983, vol. 3, p. 1025.
15. J. Petit, B. Bouchet, C. Goss, and J. de Fouguet: *Fracture, Proc. 4th Int. Conf. on Fracture (ICF4)*, D. M. R. Taplin, ed., University of Waterloo Press, Waterloo, Canada, 1977, vol. 2, p. 867.
16. M. D. Holliday and C. J. Beevers: *Int. J. of Fracture*, 1979, vol. 15, p. R27.
17. A. K. Vasudévan and S. Suresh: *Metall. Trans. A*, 1982, vol. 13A, p. 2271.
18. B. R. Kirby and C. J. Beevers: *Fatigue of Eng. Mat. and Structures*, 1979, vol. 1, p. 203.
19. S. Suresh: *Metall. Trans. A*, 1983, vol. 14A, p. 2375.